ESMO IMMUNO-ONCOLOGY VIRTUAL CONGRESS
9-12 DECEMBER 2020

#88P Identification of Prognostic Radio-Immune-Genetic Profiles in Patients Affected by Glioblastoma

Giulia Mazzaschi[1], Alessandro Olivari[1], Silvia Dall'Asta[1], Costanza Annamaria Lagrasta[1], Caterina Frati[1], Denise Madeddu[1], Antonio Pavarani[2], Marcello Tiseo[1], Maria Michiara[3], Federico Quaini[1], Pellegrino Crafa[1]
From the Department of Medicine and Surgery: [1]Medical Oncology Unit; [2] Pathology Unit; [3] Neuroradiology Unit, and [4] Hematology and Bone Marrow Transplantation Unit- University Hospital of Parma, Parma, Italy

Background: Multidisciplinary approaches may intercept the critical events implicated in dismal prognosis and limited therapeutic sensitivity of glioblastoma (GBM). Thus, we sought to integrate molecular, immunophenotypic and radiologic parameters to provide prognostic keys dissecting the clinical outcome of GBM patients.

Methods: We enrolled 57 histologically proven GBM patients whose complete clinical records, presurgical MRI and key genetic alterations were available. From 3T MRI sequences, SD Fluid Attenuated Inversion Recovery (FLAIR) and SD and Mean Apparent Diffusion Coefficient (ADC) were extracted and quantified through a software assisted texture analysis. Tumor Immune Microenvironment (TIME) was assessed by the immunohistochemical analysis of PD-L1 and the number and distribution of CD3+, CD4+, CD8+ Tumor Infiltrating Lymphocytes (TILs) and CD163+ Tumor Associated Macrophages (TAM).

Patient Population

		n: 57	
Age at diagnosis, years (median | range)		64 | 41-82	
		n	%
Sex	Male	33	57.9
	Female	24	42.1
Primary tumor site	Frontal	26	45.6
	Temporal	20	35.1
	Parietal	5	8.8
	Occipital	4	7
	Cerebellar	1	1.8
	Deep	1	1.8
Number of lesions	Single	45	78.9
	Multiple	12	21.1
IDH1 status	WT	3	87
	Mutant	50	5.3
	Missing	4	7
EGFR	WT	25	43.8
	Overexpressed	32	56.1
p53	WT	35	61.4
	Mutated	25	43.8
MGMT	Methylated	26	45.6
	Not Methylated	31	54.4
Ki67, % (median |range)		30|10-70	

Magnetic Resonance Imaging (MRI)

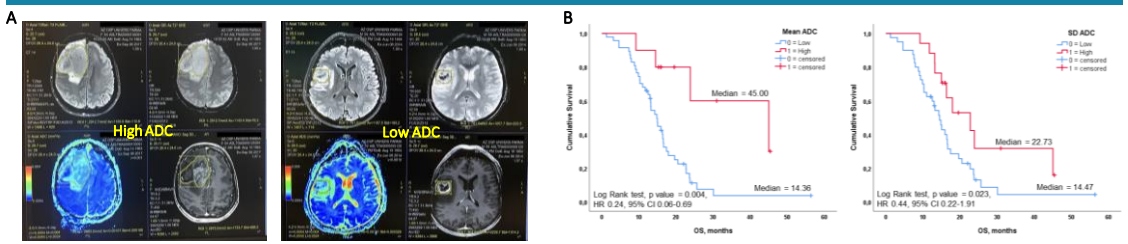

Figure 3. A: MRI images illustrating the radiologic approach followed for texture analysis. Four sequences were simultaneously compared: Fluid Attenuated Inversion Recovery (FLAIR), Gradient Echo (GRE), Apparent Diffusion Coefficient (ADC) map and T1-post Gadolinium contrast. The region of interest (ROI), outlined in yellow, manually drawn on T1-post Gadolinium slice, was automatically cloned by imaging software on the other 3 sequences to extract and quantify SD FLAIR, SD ADC and mean ADC. Two representative MRI examples of GBM cases displaying high (left) or low (right) ADC are shown. **B:** Kaplan Meier analysis documenting the positive impact of high mean (left) and SD (right) ADC on overall survival (OS) in GBM patients.

Tumor Immune Microenvironment (TIME)

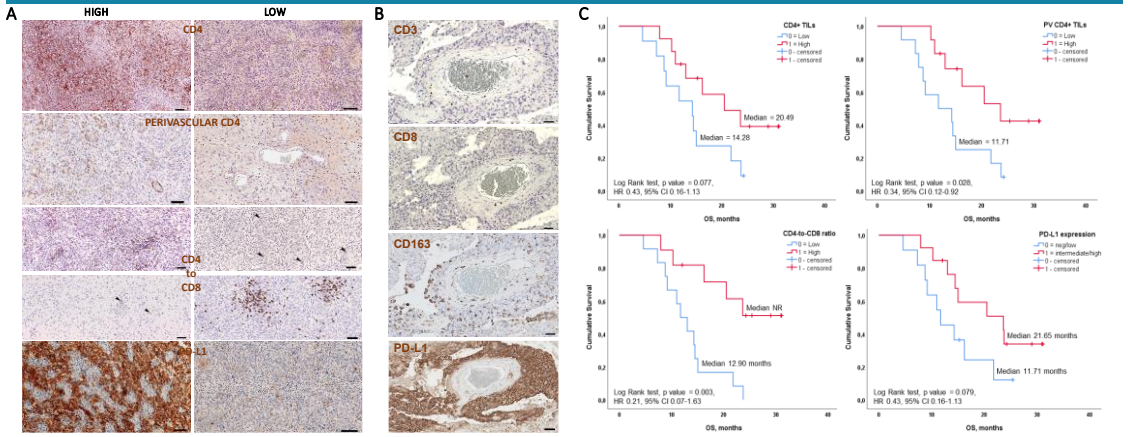

Figure 2. A: Representative images of immunoperoxidase stained sections of GBM to illustrate in sequence (top-bottom) the different extent of intratumor and perivascular (PV) CD4+ Tumor Infiltrating Lymphocytes (TILs), CD4-to-CD8 ratio and PD-L1 expression. Scale Bars: 100μm except for CD4-to-CD8 (50μm). **B:** serial sections of a GBM sample illustrating by immunoperoxidase in the same tissue area the periarteriolar immune context composed of CD3+ and CD8+ lymphocytes, CD163+ TAM and PD-L1+ cancer cells insidiously surrounding the vascular wall. Scale Bars: 50 μm. **C:** the positive impact of high number of total and PV CD4+, CD4/CD8 TILs and PD-L1 score on OS in GBM patients is shown by respective Kaplan Meier curves. Cutoffs to define high and low were established by CART tree analysis. Statistical values are inscribed in each graph.

Genetic-molecular Background

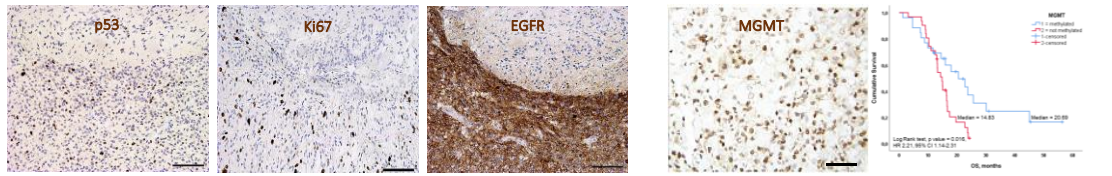

Figure 1. Serial sections from a surgically removed glioblastoma (GBM) stained by immunoperoxidase to illustrate in the same area the nuclear expression of p53 and Ki67 and the cytoplasmic/surface expression of Epidermal Growth Factor Receptor (EGFR). The neoplastic front invading the spared brain is highlighted by the sharp differential staining intensity of the three makers in cancer cells. MGMT immunostaining is shown at higher magnification on the right. Scale Bars: 100μm. Kaplan-Meier curve documents the significant impact of MGMT methylation on OS in the entire cohort of 57 GBM.

Radio-immune-genetic correlations

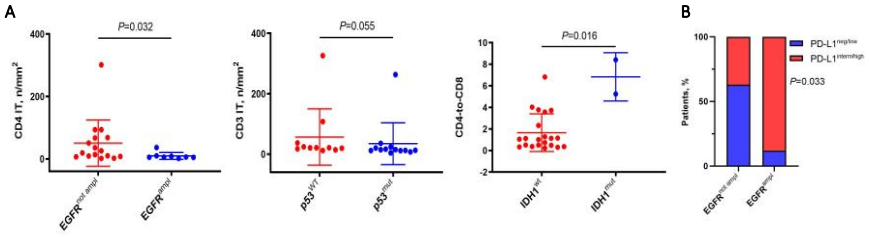

Figure 4. A: Whisker graphs of the quantitative distribution of TILs phenotypes according to genetic backgrounds, documenting the association of EGFR amplification and p53 mutation with lower number of intratumor (IT) CD3 and CD4 lymphocytes, respectively. Conversely, IDH1 mutation appears to condition a lower CD4-to-CD8 ratio. **B:** stacked bar charts showing the distribution of PD-L1 score values in GBM patients according to EGFR status. A higher fraction of GBM patients displaying intermediate-high (interm/high) PD-L1 score was documented in samples with EGFR amplification.

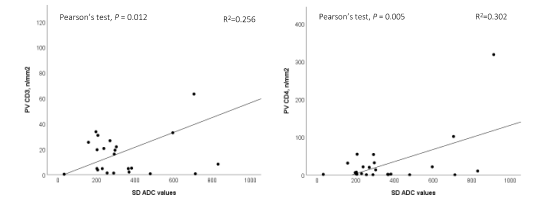

Figure 5: Scatter plot graphs illustrating the direct correlation between MRI derived quantitative SD ADC and the number of perivascular (PV) CD3 (right) and CD4 (left) TILs. Statistical significance according to linear regression (R^2) coefficient and Pearson's test are inscribed in each graph.

Integration of radio-immune-genetic features

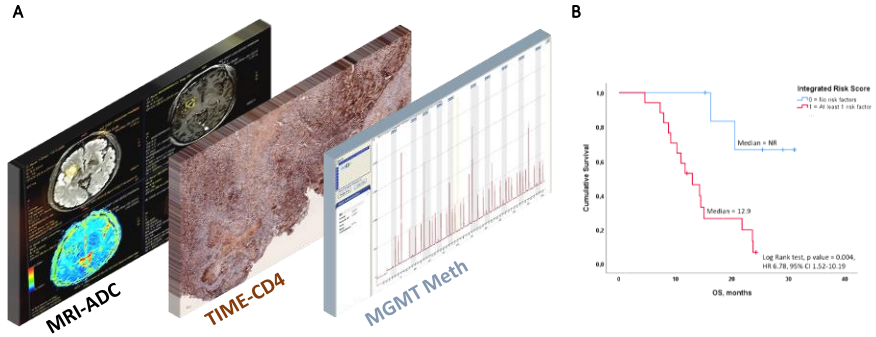

Figure 6. A: Schematic approach for the identification of risk scores in GBM patients based on the integration of predetermined prognostically relevant MRI (mean ADC), TIME (number of perivascular CD4+ TILs) and genetic (MGMT methylation status) parameters. **B**: Kaplan Meier curve documenting the impact on OS of our radio-immune-genetic score. Low mean ADC, low number of PV CD4+TILs and not methylated MGMT were considered as risk factors. The presence of at least one risk factor conditioned a mean OS of 12.9 months (...) while in GBM cases displaying mean ADC^{high}, PV CD4+^{high} and MGMT^{meth} OS was not reached.

Conclusions

Integrating radio-immune-genetic features may provide highly significant prognostic scores in GBM.

giulia.mazzaschi@studenti.unipr.it